

# Lawrence Berkeley National Laboratory

## Lawrence Berkeley National Laboratory

**Title**

Soft X-ray Image Plane Holographic Microscopy

**Permalink**

<https://escholarship.org/uc/item/7304g5jc>

**Author**

Nejdl, Jaroslav

**Publication Date**

2013-09-30

# Soft X-Ray Image Plane Holographic Microscopy

J. Nejd, <sup>1,4</sup> I. D. Howlett, <sup>1,2</sup> D. Carlton <sup>1,3</sup>, E.H. Anderson, <sup>1,3</sup> W. Chao, <sup>1,3</sup> M. C. Marconi, <sup>1,2</sup>  
J. J. Rocca, <sup>1,2</sup> and C. S. Menoni <sup>1,2,\*</sup>

<sup>1</sup> National Science Foundation Engineering Research Center for Extreme Ultraviolet Science and Technology

<sup>2</sup> Electrical and Computer Engineering, Colorado State University, Fort Collins, USA

<sup>3</sup> Center for X-Ray Optics, Lawrence Berkeley National Laboratory

<sup>4</sup> FNSPE, Czech Technical University in Prague, Brehova 7, Prague 115 19, Czech Republic

**Abstract:** Image plane holographic microscopy is demonstrated combining coherent illumination from a compact 46.9 nm wavelength laser with Fresnel zone plate optics. The method enables imaging of low absorption samples with high resolution.

Image Plane Holographic Microscopy (IPHM) is a powerful imaging method in that it enables to obtain both the phase and the amplitude of the object's wave, thereby extending the capabilities of classical microscopy that only records intensity information. IPHM is particularly attractive for imaging applications that suffer from poor absorption contrast, as it occurs in the soft x-ray when the photon energy is outside specific atomic resonances. Unlike phase contrast microscopy, IPHM allows for quantitative measurements of the electric field phasor at the image plane [1,2].

We demonstrate IPHM at soft x-ray (SXR) wavelengths using a set up that combines the coherent output from a 46.9 nm wavelength compact laser with free standing Fresnel Zone Plates (FZP) [3,4]. In IPHM the object wave is made to interfere with a reference beam to create at the detector plane an interference pattern from which the amplitude and phase of the object wave electric field phasor are obtained. Our implementation of IPHM, shown in Fig. 1, uses the same microscope configuration employed for sequential SXR imaging with the addition of a second condenser FZP that generates the reference beam [5]. The output beam from a Ne-like Ar capillary discharge laser consisting of pulses of wavelength  $\lambda=46.9$  nm, and  $\sim 0.1$  mJ energy [6] illuminates a Schwarzschild condenser, creating a convergent wavefront that illuminates a FZP placed downstream. The zero order of this FZP propagates through the optical system as the reference beam. The first order diffraction creates the object beam that is focused by the objective zone plate (OZP) near the vicinity of the reference beam focus. This ensures both the efficient illumination of the sample and the same wave-front curvature for both the reference and object beams at the detector

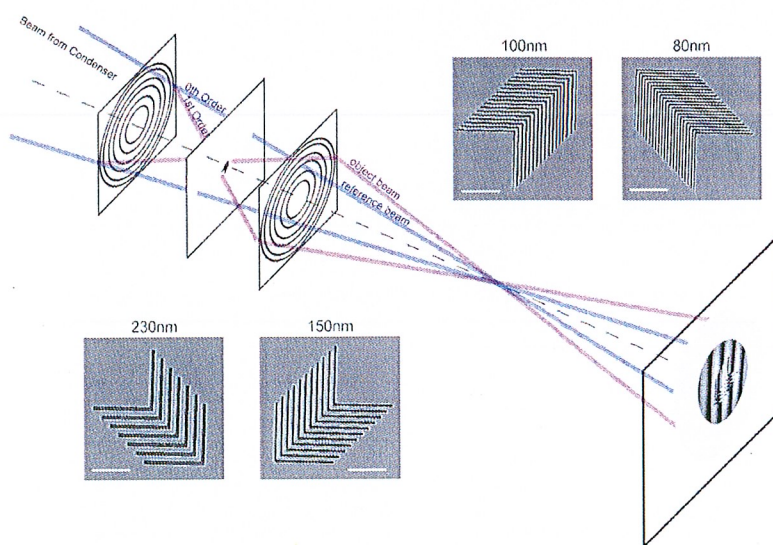


Figure 1. Schematic of Image Plane Holographic Microscopy at  $\lambda=46.9$  nm. Scanning electron microscope images of the Si elbow patterns on the image are shown.



plane. The interference pattern created at and captured by an array detector at the image plane is the image plane hologram of the object. The sample used for IPHM consists of elbow patterns with 80, 100, 150 and 230 nm dense lines fabricated on Si layer 100 nm thick. The absorption of the 100 nm Si lines is 30% at  $\lambda=46.9$  nm [7].

A hologram from the Si elbow pattern with 230 nm dense lines obtained using a 0.23NA OZP is shown in Fig. 2. The hologram was reconstructed using the Fourier transform technique, where applying a carefully designed band-pass filter centered at the carrier frequency (mean spatial frequency of interference fringes), allowed for extraction of the phase and the amplitude of the hologram, also shown in Fig. 2 [8]. The spatial resolution of the hologram image is given by the cut-off frequency of the OZP, 150 nm. A phase histogram of an area of  $40 \mu\text{m}^2$  in the phase image showed the phase difference is  $(2.3 \pm 0.3)$  rad. Using the tabulated index of refraction of Si,  $(1-\delta)=0.83$  [7], the thickness of the elbow lines is calculated to be  $(100 \pm 15)$  nm which is in good agreement with the sample specifications.

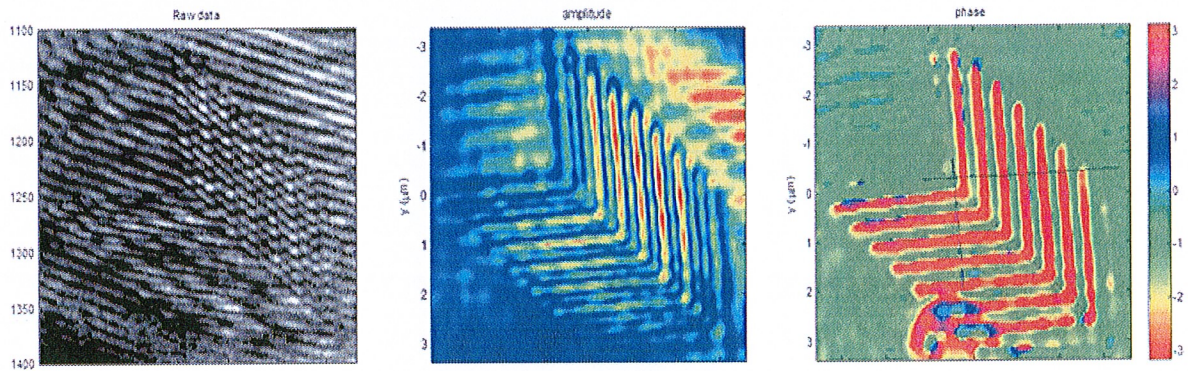


Figure 2. (From left to right) Hologram of the Si elbow pattern with 230nm dense lines recorded with a 0.23 NA OZP; amplitude of the object wave and phase obtained from the fringe phase shift.

Increasing the OZP numerical aperture to 0.46NA produced high quality holographic images of the 150 nm dense lines elbow pattern. From a histogram of the phase over an area of  $3 \mu\text{m}^2$ , a phase difference of  $(2.9 \pm 0.6)$  rad was measured, which is in agreement with the results of Fig. 2. We modeled the results to analyze the contributions to image quality from inhomogeneities in the reference beam, and from the spatial the temporal coherence of the illumination. The analysis showed that for the  $\lambda=46.9$  nm SXR laser illumination which has a coherence length of  $750 \mu\text{m}$  [9], and a coherence radius of  $375$  ( $280$ )  $\mu\text{m}$  for the 0.23NA (0.48NA) OZP, the inhomogeneities in the reference beam due to the higher diffraction orders of the FZPs, deteriorate fringe contrast.

The ability to extract amplitude and phase the image plane holograms with a simple microscope set up, demonstrated from our experiment, offers several advantages when imaging at SXR wavelengths: 1) it enhances image quality allowing to resolve regions with small variations in the absorption at the illumination wavelength; and 2) it enables to extract a two dimensional map of variations in the sample refractive index, and in turn detect inhomogeneities or defects buried within a sample. The IPHM method demonstrated in this work can be readily extended to shorter wavelengths using illumination from SXR lasers operating down to  $7.36$  nm [10].

Work supported by the NSF Engineering Research Center Program through grant EEC 0310717.

1. T. Wilhein, B. Kaulich, and J. Susini, "Two zone plate interference contrast microscopy at 4 keV photon energy," *Optics Communications*, **193**, 19, (2001).
2. A. Sakdinawat and Y. Liu, "Phase contrast soft x-ray microscopy using Zernike zone plates," *Optics Express*, **16**, 1559, (2008).
3. B.R. Benware, C.D. Macchietto, C.H. Moreno, and J.J. Rocca, "Demonstration of a High Average Power Tabletop Soft X-Ray Laser", *Physical Review Letters* **81**, 5804, (1998).
4. E.H. Anderson, *Specialized electron beam nanolithography for EUV and X-ray diffractive optics*. IEEE J. Quantum Electronics, **42**, 27, 2006.
5. S. Carbajo, I.D. Howlett, F. Brizuela, K.S. Buchanan, M.C. Marconi, W.L. Chao, E.H. Anderson, I. Artiukov, A. Vinogradov, J.J. Rocca, CS Menoni "Sequential single-shot imaging of nanoscale dynamic interactions with a table-top soft x-ray laser," *Opt. Letters*, **37**, 2994, (2012).
6. C.D. Macchietto, B.R. Benware, and J.J. Rocca, "Generation of millijoule-level soft-x-ray laser pulses at a 4-Hz repetition rate in a highly saturated tabletop capillary discharge amplifier," *Optics Letters* **24**, 1115, (1999).
7. Center for X-Ray Optics, Lawrence Berkeley National Laboratory, <http://www.cxro.lbl.gov/>
8. M. Takeda, H. Ina, and S. Kobayashi, "Fourier-transform method of fringe-pattern analysis for computer-based topography and interferometry," *J. Opt. Soc. Amer.*, **72**, 156, (1982).
9. L. Urbanski, M. C. Marconi, L. M. Meng, M. Berrill, O. Guilbaud, A. Klisnick, and J. J. Rocca, "Spectral linewidth of a Ne-like Ar capillary discharge soft-x-ray laser and its dependence on amplification beyond gain saturation," *Phys. Rev. A*, **85**, 033837 (2012).
10. D. Alessi, Y. Wang, B.M. Luther, L. Yin, D.H. Martz, M.R. Woolston, Y. Liu, M. Berrill, J.J. Rocca "Efficient Excitation of Gain-Saturated Sub-9-nm-Wavelength Tabletop Soft-X-Ray Lasers and Lasing Down to 7.36 nm". *Phys. Rev. X*, **1**, 021023 (2011).

## **DISCLAIMER**

This document was prepared as an account of work sponsored by the United States Government. While this document is believed to contain correct information, neither the United States Government nor any agency thereof, nor The Regents of the University of California, nor any of their employees, makes any warranty, express or implied, or assumes any legal responsibility for the accuracy, completeness, or usefulness of any information, apparatus, product, or process disclosed, or represents that its use would not infringe privately owned rights. Reference herein to any specific commercial product, process, or service by its trade name, trademark, manufacturer, or otherwise, does not necessarily constitute or imply its endorsement, recommendation, or favoring by the United States Government or any agency thereof, or The Regents of the University of California. The views and opinions of authors expressed herein do not necessarily state or reflect those of the United States Government or any agency thereof or The Regents of the University of California.

This work was supported by the Director, Office of Science, of the U.S. Department of Energy under Contract No. DE-AC02-05CH11231.